

## Letter

## Emergence of extreme events from randomly chirped condensate

Saad Alhadlaq<sup>a,\*</sup>, Sergey A. Ponomarenko<sup>a,b</sup><sup>a</sup> Department of Electrical and Computer Engineering, Dalhousie University, Halifax, B3J 2X4, Nova Scotia, Canada<sup>b</sup> Department of Physics and Atmospheric Science, Dalhousie University, Halifax, B3H 4R2, Nova Scotia, Canada

## ARTICLE INFO

Communicated by B. Malomed

## Keywords:

Modulation instability

Rogue waves

NLSE

Random chirp

## ABSTRACT

We explore rogue wave emergence in generic wave systems governed by the nonlinear Schrödinger equation. We highlight the interplay between the stochastic focusing induced by a random chirp of a continuous wave condensate and modulation instability of the condensate to periodic and/or random perturbations. We show that regardless of its statistical properties, the random chirp of the condensate leads to a non-Gaussian, heavy-tailed probability density distribution of peak powers of the waves excited atop of the condensate, which is a statistical signature of rogue waves, or more broadly, extreme events in physics.

## 1. Introduction

The original, and rightfully dreaded, ocean rogue waves manifest themselves as the waves of unusually high amplitudes, and therefore destructive power, on the surface of deep water [1]; rogue waves have a statistical nature because they occur randomly, yet more often than is anticipated by generic Gaussian statistics. Hence, the non-Gaussian statistics of rogue waves can be considered their most fundamental signature that allows us to extrapolate to a broader class of extreme event phenomena which need not be even waves [2].

To date, extreme events have been discovered in the areas of physics as diverse as optics and condensed matter physics [3]. Most work on the extreme event appearance in nonlinear wave systems has focused on rogue wave excitation through modulation instability (MI) of a continuous wave background [4,5], although different emergence scenarios can be envisioned in the supercontinuum generation in optical fibers [6], or in resonant systems [7,8]. In a standard setting, extreme events spring from a uniform background unstable to MI which is typically induced by statistically stationary, localized additive noise [9,10].

In most realistic situations, however, there exists an external driving source such as random impurities in optical and/or matter wave systems, or random bursts of wind in the case of ocean rogue waves. We conjecture that under favorable conditions, the external driving acts in concert with MI to facilitate extreme event excitation in nonlinear wave systems. This can become particularly pronounced if the external factors cause random focusing of the waves, thereby further promoting high-amplitude wave events.

In this work, we test this hypothesis by considering waves described within the framework of the nonlinear Schrödinger equation (NLSE), which applies generically to weakly nonlinear, weakly dispersive wave systems of any physical nature [11]. Instructively, the NLSE serves as a basis for the now-well-recognized mathematical analogy between rogue waves in deep ocean and in optical fibers [12]. To set the stage, we first briefly examine completely deterministic solutions to NLSE arising from MI of a constant background with neither additive nor multiplicative noise present. Next, we proceed to examine a more realistic model of a condensate with a randomly perturbed amplitude (additive noise) and a random overall phase chirp (multiplicative noise). Although, numerous past research has been concerned with the role of initial conditions for RW formation [3,6,13,14], including partially coherent input waves [15], as well as various forms of random perturbations of the condensate [6,16–19], we stress that the concept of multiplicative noise manifested by an overall random chirp of the condensate has been largely unexplored to date. It is worth mentioning that the effects of deterministic linear gain/loss on the extreme event generation were studied in [20]. In the short-term limit, such a gain/loss term in the NLSE can be viewed as mathematically equivalent to the presence of a linear chirp of the condensate. However, there are two key differences between the approach of [20] and this work. First, an NLSE with linear gain/loss is equivalent to the standard conservative NLSE, describing the evolution of a linearly chirped condensate, only for a specific time—or propagation distance in the optical case—dependence of the effective nonlinearity coefficient; this is a common feature of integrable open systems governed by inhomogeneous NLSEs [21]. Second, and most important, while the authors of Ref. [20] consider determin-

\* Corresponding author.

E-mail address: [s.alhadlaq@dal.ca](mailto:s.alhadlaq@dal.ca) (S. Alhadlaq).

istic driving only, our approach makes it possible to explore random driving. In this sense, we argue that the introduced multiplicative noise incorporates, to some extent, the effects of random external driving. We determine the probability density function (PDF) of peak powers of the waves excited by such randomly driven MI and demonstrate that, indeed, the PDF becomes strongly non-Gaussian irrespective of the origin and statistical nature of the multiplicative noise, thereby underscoring the universality of our findings.

## 2. Theoretical formulation

We consider the nonlinear Schrodinger equation (NLSE) governing the evolution of an optical pulse/water wave envelope  $\Psi$ . The NLSE can be expressed in the dimensional form as

$$i\partial_{\zeta}\Psi - \frac{\beta_2}{2}\partial_{\tau\tau}^2\Psi + \gamma|\Psi|^2\Psi = 0. \quad (1)$$

Here, in the context of optical pulses in fibers to be specific,  $\beta_2$  is the group velocity dispersion (GVD) in  $ps^2 km^{-1}$  and  $\gamma$  is a nonlinearity coefficient in  $W^{-1} km^{-1}$ . Further,  $\zeta$  and  $\tau$  refer to the propagation distance and time in the reference frame moving with the group velocity of the pulse, respectively. In the anomalous dispersion regime,  $\beta_2 < 0$  which is the parameter regime of interest to us throughout this work.

We study two sets of initial conditions. First, we introduce a deterministic initial condition corresponding to a periodically perturbed, chirped condensate by the expression

$$\Psi(\tau, 0) = \sqrt{P_0}(1 + \varepsilon \cos \omega\tau) \exp(-iC\tau^2/2). \quad (2)$$

Here  $P_0$  is a power of the condensate (cw background),  $C$  is a condensate chirp parameter,  $\varepsilon$  and  $\omega$  are the modulation depth and frequency of the harmonic perturbation, respectively; we stress that all parameters are purely deterministic here. We note that we chose a generic quadratic phase of the condensate which triggers focusing or spreading, depending on the sign of the chirp. The situation is analogous to a thin lens that imposes a quadratic spatial phase on an incident beam. The latter is then either focused or defocused depending on the sign of the focal length [22]; the temporal lens formally works the same way due to the space-time duality of beam diffraction in free space and pulse spreading in a dispersive medium [23]. Although the phase of a realistic fluctuating condensate field can have a complicated dependence on time, the generic quadratic phase approximation qualitatively captures the essence of additional focusing that, in conjunction with MI, promotes extreme event occurrence in such a condensate. We then examine the latter which gives rise to the following initial condition:

$$\Psi(\tau, 0) = \sqrt{P_0}[1 + \varepsilon f(\tau)] \exp(-iC\tau^2/2); \quad f^*(\tau) = f(\tau), \quad (3)$$

where  $f(\tau)$  is a random amplitude perturbation and  $C$  is a random chirp. The amplitude perturbation is a zero-mean Gaussian random process which can be modeled by a sufficient number  $N$  of uncorrelated harmonics

$$f(\tau) = \frac{1}{N} \sum_{n=1}^N \cos \omega_n \tau, \quad (4)$$

with a set of random frequencies  $\{\omega_n\}$ . We consider several statistical models for random chirp.

## 3. Numerical simulations

To be specific, we perform numerical simulations for pulses in a standard single-mode silica glass fiber. Importantly, we operate within the MI range to ensure that the rogue waves are triggered in the system. The modulation instability gain, determined through the linear stability analysis against small perturbations, reads [24]

$$G_{MI}(\omega) = |\beta_2 \omega| \sqrt{\frac{4}{|\beta_2| L_{NL}} - \omega^2}, \quad (5)$$

**Table 1**

Parameter values implemented in the simulation of a single-mode optical fiber operating at 1550 nm.

| Parameter                | Symbol    | Value | Unit             |
|--------------------------|-----------|-------|------------------|
| GVD                      | $\beta_2$ | -20   | $ps^2 km^{-1}$   |
| Nonlinearity coefficient | $\gamma$  | 1.1   | $W^{-1} km^{-1}$ |
| Power                    | $P_0$     | 30    | $W$              |
| Characteristic NL length | $L_{NL}$  | 30.3  | $m$              |

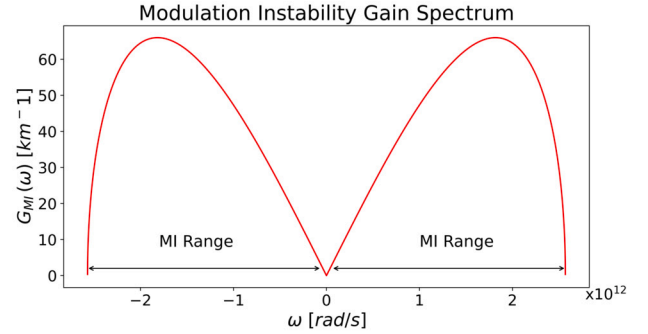


**Fig. 1.** Modulation instability gain spectrum given by Eq. (5) and displayed for the parameter values listed in Table 1. The MI range is indicated with the double ended arrows.

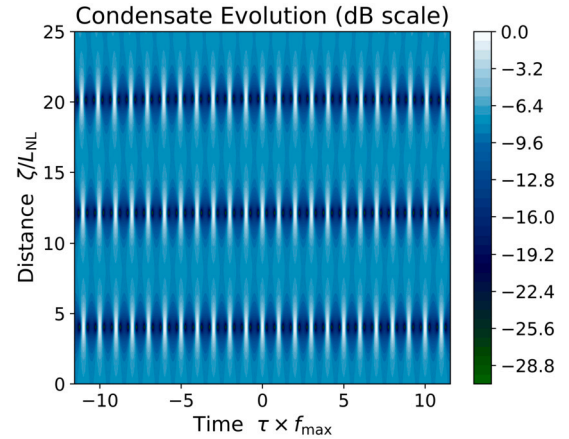


**Fig. 2.** Intensity profile of a chirpless condensate at the nonlinear stage of MI evolution in the silica glass fiber. The intensity is given in a dB scale. The parameter values are given in Table 1.

where we defined a characteristic nonlinear length  $L_{NL} = (\gamma P_0)^{-1}$ . The MI gain maximum corresponds to the frequency  $\omega_{max} = \sqrt{2/(|\beta_2| L_{NL})}$ . Accordingly, we show the range of simulation parameters employed in our model in Table 1.

Using these parameters, we can depict the MI gain in Fig. 1. It follows that the latter is constrained to the frequency range of up to approximately 400 GHz. While within this range and keeping the modulation depth to be  $\varepsilon = 0.05$ , we present our results for the deterministic and random condensates. We stress that throughout our simulations we work with a dimensionless chirp parameter  $C_0$  which is obtained by scaling the actual chirp  $C$  to the frequency of maximum MI gain such that  $C = C_0 * f_{max}$ , where  $f_{max} = \omega_{max}/2\pi$ .

We first study the deterministic initial conditions by numerically solving Eq. (1) subject to Eq. (2) in the chirpless case,  $C = 0$ . In Fig. 2, we exhibit the simulated envelope evolution along the fiber. We obtain a train of Akhmediev breathers at the nonlinear stage of MI in complete agreement with the earlier work [25] in the same parameter range. Next, introducing a nonzero chirp into the initial conditions, we observe that the MI evolution scenario is drastically modified. Indeed, we can

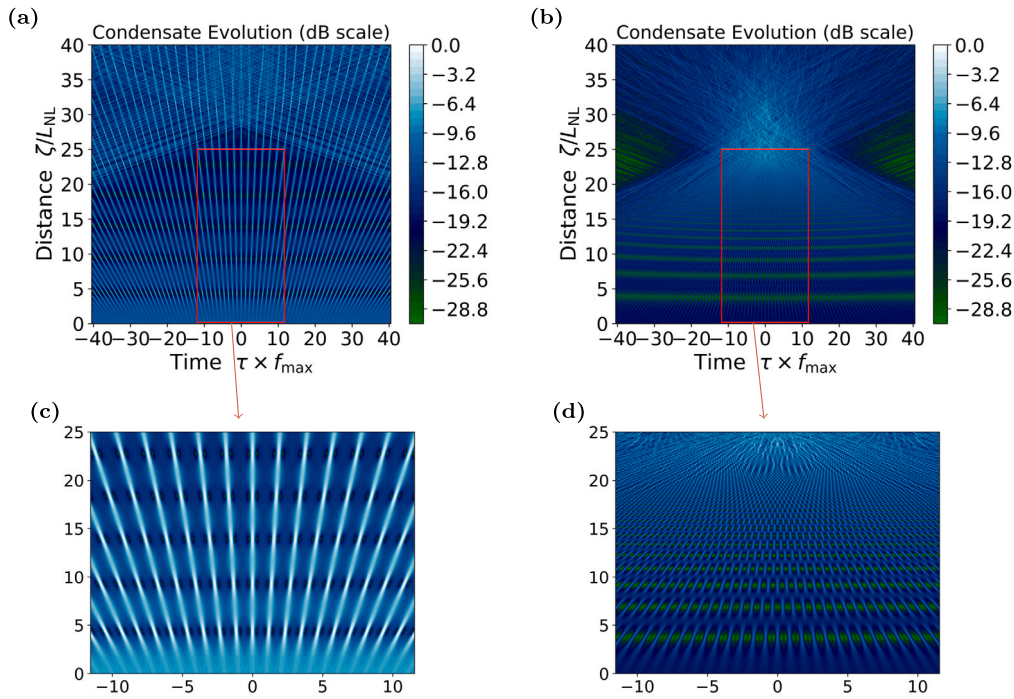


**Fig. 3.** Chirped condensate evolution for (a)  $C_0 = -0.75$  (negative chirp) showing spreading of the condensate, (b)  $C_0 = 0.75$  (positive chirp) revealing focusing of an Akhmediev breather train formed over sufficiently short propagation distances. The parameter values are given in Table 1, (c) and (d) are magnified versions of the portions within red boxes to illustrate fine scale effects of the chirp.

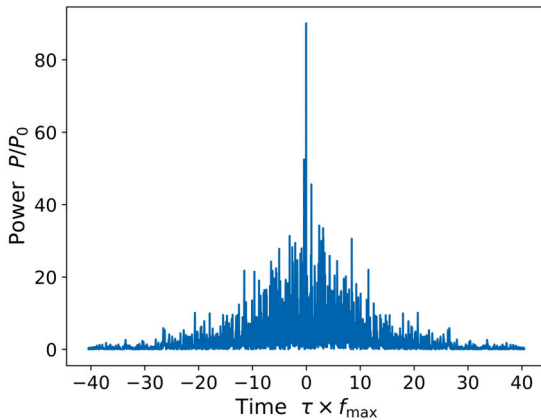


**Fig. 4.** Field power distribution of the condensate as a function of time in the focal region with additional focusing imposed by a positive chirp.

infer from Fig. 3 that depending on the sign of the chirp, the condensate either spreads out (defocussing induced by the negative chirp) or Akhmediev breathers sharply focus (positive chirp) even for relatively modest magnitudes of the dimensionless chirp  $C_0$ .

A closer look at the results in Fig. 3a reveals that in the negative chirp case, any intensity bump atop the background spreads out so quickly that Akhmediev breathers cannot even form, implying that such a chirp can inhibit extreme event excitation. On the other hand, we can infer from Fig. 3b that while a classic Akhmediev breather train forms over short enough propagation distances, the positive chirp drastically alters the long-term MI evolution scenario.

Specifically, we observe substantial focusing that culminates in the emergence of massive amplitude waves carrying powers in excess of 80 times that of the input condensate. In Fig. 4, we exhibit a representative example of the field power distribution of the condensate within the focusing region where the peak power sharply increases due to a positive chirp as is visible in Fig. 3b.

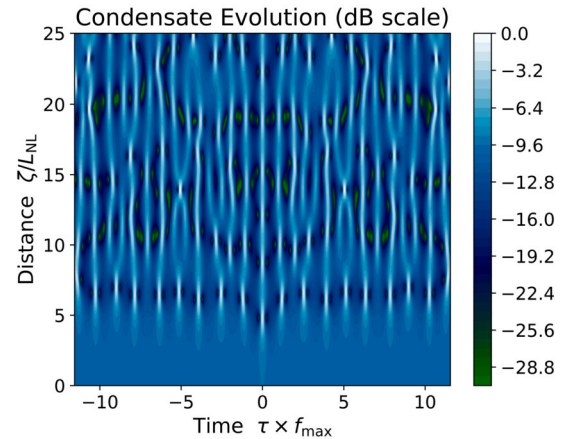


**Fig. 5.** Nonlinear stage of the MI evolution of a randomly perturbed, chirpless condensate. The parameter values are given in Table 1.

Next, consider random initial conditions, Eqs. (3) and (4), to illustrate the MI evolution of randomly driven condensate. To this end, we first display the nonlinear evolution stage of randomly perturbed, chirpless condensate in Fig. 5. We can infer from the figure that the random MI evolution greatly resembles the deterministic one, except the train of perfectly periodic Akhmediev breathers is replaced with a random sea of colliding solitons riding atop of the condensate.

We are now in a position to examine the statistics of peak powers of said solitons emerging on the background. To this end, we have studied several statistical models of the chirp. The first model corresponds to an exponential distribution of the chirp [26] defined as

$$P(C_0) = \begin{cases} \frac{1}{\langle C_0 \rangle} \exp(-C_0/\langle C_0 \rangle); & C_0 \geq 0, \\ 0, & C_0 < 0, \end{cases} \quad (6)$$

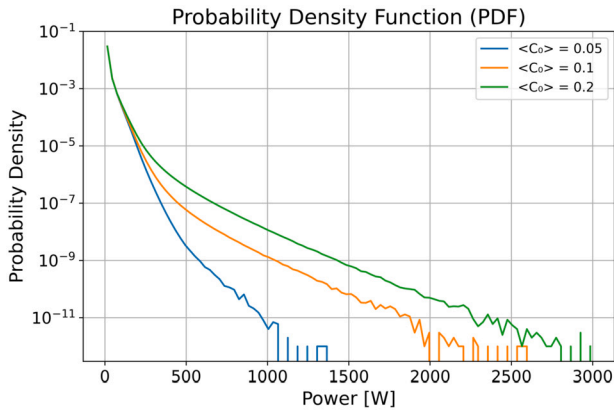


**Fig. 6.** Peak power PDF of an ensemble of 1000 chirped condensate realizations with exponentially distributed chirp. The chirp distribution is completely determined by the average chirp  $\langle C_0 \rangle$  shown in the legend. The parameter values are given in Table 1.

where the angle brackets denote ensemble averaging. Such a chirp distribution can accidentally occur in localized areas of the ocean where the wind gusts favor a certain set of directions over the others, resulting in a net focusing effect for the waves. At the same time, a similar distribution can be engineered in optical fibers by employing linear [27] or quadratic [28] electro-optical effect with a fluctuating control field of slow (microwave) frequency to realize a time lens [23]. In Fig. 6 we show the probability density function (PDF) of peak powers of the wave envelopes propagating in the fiber for three values of the average chirp of the condensate. All PDFs are shown in the logarithmic scale so that any deviation from a straight line signifies non-Gaussian statistics. The results clearly show that the higher the average condensate chirp, the longer the PDF tail, and hence the greater the chance of finding waves with extremely high peak powers; as well, in all three cases the PDFs differ from a straight line showing unambiguous signatures of extreme event emergence.

At this stage, one may wonder whether a chirped condensate model not statistically favoring positive over negative chirps would be more realistic: After all, the wind gusts in the ocean randomly change their direction over short spans of time and random fiber impurities can equally likely up-chirp or down-chirp a traveling pulse. To remove the sign chirp bias, we alternatively model the chirp as a random telegraph process so that the chirp can take on just two values  $a$  and  $-a$  and switch from one to the other randomly. The mathematical representation of this process can be expressed in the form of a state transition matrix [29] as follows:

$$P = \begin{bmatrix} p_{11} & p_{12} \\ p_{21} & p_{22} \end{bmatrix}, \quad (7)$$

where

$$p_{ij} = P(X_{m+1} = j \mid X_m = i) \quad \text{for } i, j \in \{1, 2\}, \quad (8)$$

and

$$\sum_{k=1}^2 p_{ik} = 1. \quad (9)$$

Here  $X_m$  is the chirp value at time  $m \in \{0, 1, 2, \dots\}$ , and  $P(X_{m+1} = j \mid X_m = i)$  is a conditional probability for the chirp to take the value of state  $j$ , given its prior state  $i$ . States  $\{1, 2\}$  refer to the alternating chirp values  $\{a, -a\}$ . We can readily realize this model on the optical table by employing the electro-optical effect mediated by a dc voltage with randomly switching polarity, for example. In Fig. 7 we display the PDF of peak powers of the waves excited at the nonlinear MI stage from such a telegraph-chirped random condensate. Instructively, the PDF in Fig. 7 is qualitatively similar to that in Fig. 6. At first glance, it might seem counter-intuitive, considering that the telegraph process does not

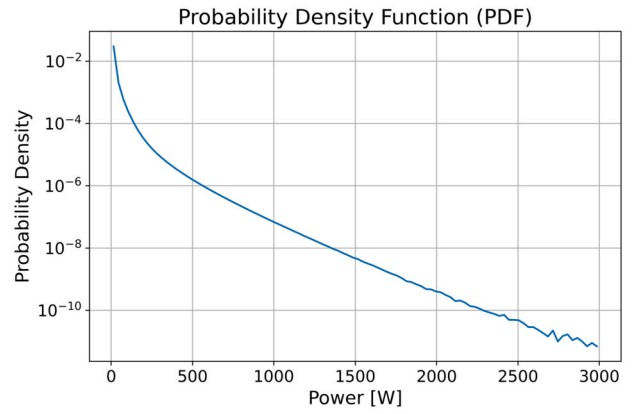


**Fig. 7.** Peak power PDF of an ensemble of 1000 chirped condensate realizations with the chirp represented by a telegraph process: The condensate chirp switches between 0.75 and -0.75 at random times. The parameter values are given in Table 1.

discriminate between positive and negative chirp values. We notice, however, that only focused ensemble members contribute to enhanced extreme event generation, while spreading ones play no role here. It is then not surprising that the telegraph-like chirped condensate promotes extreme events just like a condensate with a continuous chirp distribution. As a final note, we mention that we have performed simulations with a multitude of other chirp distribution models all of which yielding the same qualitative result: Chirping the condensate skews the PDF tail toward high power events, making our findings generic.

#### 4. Summary

The nonlinear regime of modulation instability of a continuous wave background (condensate) sets the stage for a number of fascinating nonlinear phenomena. Although the emergence of rogue waves from the condensate due to MI has been widely studied to date [24,30–37], the MI of a condensate stirred by random external perturbations has not been carefully examined yet. In this work, we have explored extreme event excitation triggered by the MI of a randomly chirped condensate. We have shown that in the case of a deterministic chirped condensate, the sign of the chirp drastically affects the evolution scenario of the nonlinear stage of MI leading to either spreading and dissipation of any perturbations arising atop of the condensate, or to strong focusing of said perturbations. Having examined a number of statistical models of the condensate chirp, we have demonstrated numerically that irrespective of the statistical nature of the condensate chirp, the mere presence of the latter promotes high power event emergence at a rate higher than that predicted by Gaussian statistics. Our results are applicable in equal measure to rogue waves in deep oceans as well as in optical fibers which are governed by the nonlinear Schrödinger equation. We stress that although modeling a generic external driving through a random condensate chirp may seem as an oversimplification, the generic character of our findings makes this model a starting point to explore a fundamental interplay between MI and random external driving that facilitates extreme event excitation in nonlinear wave systems.

#### CRediT authorship contribution statement

**Saad Alhadlaq:** Writing – review & editing, Writing – original draft, Software, Formal analysis. **Sergey A. Ponomarenko:** Writing – review & editing, Writing – original draft, Supervision, Funding acquisition, Conceptualization.



## Declaration of competing interest

The authors declare that they have no known competing financial interests or personal relationships that could have appeared to influence the work reported in this paper.

## Data availability

No data was used for the research described in the article.

## Acknowledgement

The authors acknowledge support from NSERC (RGPIN-2018-05497, CREATE 528099-2019).

## References

- [1] C. Kharif, E. Pelinovsky, A. Slunyaev, *Rogue Waves in the Ocean*, Springer Science & Business Media, 2008.
- [2] D.T. Jenks, T.D. Coates, L. Wald, *Hyperwave Theory: The Rogue Waves of Financial Markets*, Archway Publishing, 2020.
- [3] M. Onorato, S. Residori, U. Bortolozzo, A. Montina, F. Arecchi, Rogue waves and their generating mechanisms in different physical contexts, *Phys. Rep.* 528 (2) (2013) 47–89.
- [4] N. Akhmediev, B. Kibler, F. Baronio, M. Belić, W.-P. Zhong, Y. Zhang, W. Chang, J.M. Soto-Crespo, P. Vouzas, P. Grelu, et al., Roadmap on optical rogue waves and extreme events, *J. Opt.* 18 (6) (2016) 063001.
- [5] L. Liu, W.-R. Sun, B.A. Malomed, Formation of rogue waves and modulational instability with zero-wavenumber gain in multicomponent systems with coherent coupling, *Phys. Rev. Lett.* 131 (9) (2023) 093801.
- [6] J.M. Dudley, F. Dias, M. Erkintalo, G. Genty, Instabilities, breathers and rogue waves in optics, *Nat. Photonics* 8 (10) (2014) 755–764.
- [7] Y.E. Monfared, S.A. Ponomarenko, Non-Gaussian statistics and optical rogue waves in stimulated Raman scattering, *Opt. Express* 25 (6) (2017) 5941–5950.
- [8] Y.E. Monfared, S.A. Ponomarenko, Non-Gaussian statistics of extreme events in stimulated Raman scattering: the role of coherent memory and source noise, *Phys. Rev. A* 96 (4) (2017) 043817.
- [9] D.S. Agafontsev, V.E. Zakharov, Integrable turbulence and formation of rogue waves, *Nonlinearity* 28 (8) (2015) 2791.
- [10] J.M. Soto-Crespo, N. Devine, N. Akhmediev, Integrable turbulence and rogue waves: breathers or solitons?, *Phys. Rev. Lett.* 116 (10) (2016) 103901.
- [11] Y.S. Kivshar, G.P. Agrawal, *Optical Solitons: from Fibers to Photonic Crystals*, Academic Press, 2003.
- [12] J.M. Dudley, G. Genty, A. Mussot, A. Chabchoub, F. Dias, Rogue waves and analogies in optics and oceanography, *Nat. Rev. Phys.* 1 (11) (2019) 675–689.
- [13] P. Walczak, S. Randoux, P. Suret, Optical rogue waves in integrable turbulence, *Phys. Rev. Lett.* 114 (14) (2015) 143903.
- [14] A. Picozzi, J. Garnier, T. Hansson, P. Suret, S. Randoux, G. Millot, D.N. Christodoulides, Optical wave turbulence: towards a unified nonequilibrium thermodynamic formulation of statistical nonlinear optics, *Phys. Rep.* 542 (1) (2014) 1–132.
- [15] P. Suret, R.E. Koussaifi, A. Tikan, C. Evain, S. Randoux, C. Szwaj, S. Bielawski, Direct observation of rogue waves in optical turbulence using time microscopy, arXiv preprint, arXiv:1603.01477, 2016.
- [16] D.R. Solli, C. Ropers, P. Koonath, B. Jalali, Optical rogue waves, *Nature* 450 (7172) (2007) 1054–1057.
- [17] A. Mussot, A. Kudlinski, M. Kolobov, E. Louvergneaux, M. Douay, M. Taki, Observation of extreme temporal events in cw-pumped supercontinuum, *Opt. Express* 17 (19) (2009) 17010–17015.
- [18] M. Erkintalo, G. Genty, J. Dudley, Rogue-wave-like characteristics in femtosecond supercontinuum generation, *Opt. Lett.* 34 (16) (2009) 2468–2470.
- [19] G. Xu, A. Chabchoub, D.E. Pelinovsky, B. Kibler, Observation of modulation instability and rogue breathers on stationary periodic waves, *Phys. Rev. Res.* 2 (3) (2020) 033528.
- [20] M. Onorato, D. Proment, Approximate rogue wave solutions of the forced and damped nonlinear Schrödinger equation for water waves, *Phys. Lett. A* 376 (45) (2012) 3057–3059.
- [21] S.A. Ponomarenko, G.P. Agrawal, Do solitonlike self-similar waves exist in nonlinear optical media?, *Phys. Rev. Lett.* 97 (1) (2006) 013901.
- [22] J.W. Goodman, *Introduction to Fourier Optics*, Roberts and Company Publishers, 2005.
- [23] B.H. Kolner, M. Nazarathy, Temporal imaging with a time lens, *Opt. Lett.* 14 (12) (1989) 630–632.
- [24] G.P. Agrawal, *Nonlinear Fiber Optics*, Academic Press, 2007.
- [25] J.M. Dudley, G. Genty, F. Dias, B. Kibler, N. Akhmediev, Modulation instability, Akhmediev breathers and continuous wave supercontinuum generation, *Opt. Express* 17 (24) (2009) 21497–21508.
- [26] O. Ibe, *Fundamentals of Applied Probability and Random Processes*, Academic Press, 2014.
- [27] F.J. Marinho, L.M. Bernardo, Graded-index time-lens implementation, *Opt. Lett.* 31 (11) (2006) 1723–1725.
- [28] M. Qasymeh, M. Cada, S.A. Ponomarenko, Quadratic electro-optic Kerr effect: applications to photonic devices, *IEEE J. Quantum Electron.* 44 (8) (2008) 740–746.
- [29] H. Pishro-Nik, *Introduction to Probability, Statistics, and Random Processes*, Kappa Research, LLC Blue Bell, PA, USA, 2014.
- [30] A.R. Osborne, *Nonlinear ocean wave and the inverse scattering transform*, in: *Scattering*, Elsevier, 2002, pp. 637–666.
- [31] V.E. Zakharov, L.A. Ostrovsky, Modulation instability: the beginning, *Phys. D: Nonlinear Phenom.* 238 (5) (2009) 540–548.
- [32] N. Akhmediev, J.M. Dudley, D.R. Solli, S.K. Turitsyn, Recent progress in investigating optical rogue waves, *J. Opt.* 15 (6) (2013) 060201.
- [33] B. Kibler, J. Fatome, C. Finot, G. Millot, F. Dias, G. Genty, N. Akhmediev, J.M. Dudley, The Peregrine soliton in nonlinear fibre optics, *Nat. Phys.* 6 (10) (2010) 790–795.
- [34] B. Kibler, J. Fatome, C. Finot, G. Millot, G. Genty, B. Wetzell, N. Akhmediev, F. Dias, J.M. Dudley, Observation of Kuznetsov-ma soliton dynamics in optical fibre, *Sci. Rep.* 2 (1) (2012) 463.
- [35] A. Chabchoub, B. Kibler, C. Finot, G. Millot, M. Onorato, J.M. Dudley, A. Babanin, The nonlinear Schrödinger equation and the propagation of weakly nonlinear waves in optical fibers and on the water surface, *Ann. Phys.* 361 (2015) 490–500.
- [36] F. Copie, S. Randoux, P. Suret, The physics of the one-dimensional nonlinear Schrödinger equation in fiber optics: rogue waves, modulation instability and self-focusing phenomena, *Rev. Phys.* 5 (2020) 100037.
- [37] V.E. Zakharov, A. Gelash, Nonlinear stage of modulation instability, *Phys. Rev. Lett.* 111 (5) (2013) 054101.